IOSR Journal of Mechanical and Civil Engineering (IOSR-JMCE)
e-ISSN: 2278-1684,p-ISSN: 2320-334X, Volume 13, Issue 4 Ver. VII (Jul. - Aug. 2016), PP 16-26
www.iosrjournals.org

Effect of Inlet-Outlet Location on Heat and Mass Removal from a Box Heterogeneously Heated From Below

Tran Van Tran[1], Nguyen Ngoc Thang[2], Nguyen Thi Thuy[1]
[1] *Hanoi University of Science, VNUH, Hanoi Vietnam,*
[2] *The university of Fire Fighting and Prevention*

***Abstract**: The purpose of this paper is to study the spreading of a contaminant accompanied with natural convection in a box heterogeneously heated from below, and to find out the effect of the inlet-outlet configuration on the removal of the contaminant and heat from the box by low air rate ventilation. This problem, in practice, relates to modeling a living room or a working place where some sources of heat and contaminant are in the simultaneous action. This model can be also applied to an enclosure where natural convection is caused by the effect that its floor is partly heated by the sunlight. In this study the box bottom is supposed to be divided into four separated parts with different boundary conditions for temperature or heat flux. An area contaminant source ("hot" or "cool' –with or without releasing heat respectively) locates in the center of the bottom side. Good knowledge of the contaminant spreading process in the box under the influence of the natural convection would be useful for setting an efficient ventilation scheme in order to remove more heat and the contaminant from the enclosure. The finite difference method based on the Samarski scheme with ADI technique as well as the multigrid method is applied for numerical simulations. The results of the simulation show that the contaminant density within the box is proportional to the intensity of the heat flux at the corresponding domain on the floor. To elucidate the effect of the inlet-outlet configuration on the heat-contaminant removal efficiency, three inlet locations marked by L (low), M (middle) and H (high) combine in pairs with three such positions of the outlet on the opposite wall are chosen. So there are totally eighteen configurations are taken for the consideration. The simulations show that the removal efficiency quite depends on the inlet-outlet arrangement as well as the direction of the ventilation flow.*

***Keywords:** box, three-dimensional, natural convection, contaminant spreading, Samarski scheme, multigrid, heterogeneous heating.*

I. Introduction

The spreading process of a contaminant accompanied by a convective motion in the air is a much known phenomenon that often occurs almost everywhere. The contaminant source may be "independent" on the heat source or they are merged together. Combustion reactions are often of the second case. In an industrial enclosure a heat source usually ejects one or several contaminant matters simultaneously. The heat convective motion as expected always makes the contaminant spreading more quick. But it is not its unique effect. In the case when the temperature or heat flux is not homogeneous on boundaries, in our case on the floor of the box, the contaminant distribution in the enclosure is strongly influenced too. This issue is the first primary study interest of this paper.

Natural convection in an enclosure caused by heating from below or the difference in temperature of the side walls has been theoretically and experimentally investigated intensively from several decades ago. This problem has been attractive for the theoretical investigation as well as application. One of the earliest studies of three-dimensional natural convection in a box with differential side heating by numerical simulation was carried out by Millinson and De Vahl Davis [1]. They revealed the steady kind of air motion for moderate Rayleigh number (*Ra*). And the motion is essentially three-dimensional. In [2] the same problem was considered for *Ra* ranged from 10^3 to 2.10^{16}. The laminar flows were observed again at not very large *Ra*. This problem was also solved experimentally in [3] for *Ra* from 10^4 to 2.10^7, and numerically by finite difference method in [4] for *Ra* not exceeded 10^6. It is interesting to note that in [5] the transition from the steady flow to the time-periodical natural convective motion in a box was observed. The natural convection considered in [6] is different from that of [1-5] by the heating way. Namely, in [6] the box is heated from below and the Rayleigh number is from 3500 to 10^4. Four different stable convective structures were recognized. Orhan Aydin and Wen-jei Yang [7] studied natural convection in a two-dimensional rectangular enclosure with localized heating from below and symmetrical cooling from the sides. Four dimensionless heat source length of 1/5, 2/5, 3/5, 4/5 were taken for numerical simulation at *Ra* from10^3 to 10^6. Recently natural convection of nanofluids has been investigated [8]. In this paper we consider the natural convection in a box caused by the non-homogeneity of the temperature or heat flux applied to different parts of the box bottom. And the way a contaminant spreads in the box in the presence of this convective motion is considered.

Ventilation of an enclosure with heat or and contaminant source is complicated but important problem. It applies not only to living or working places to create good air quality but also to many industrial objects from such small as an electronic chip to a huge factory. So in the last decades a lot of works have been done in this field. These studies mainly include the constructing model, proposing the methods of solution and a lot of specified numerical simulations. One of the early experimental studies is provided in [9] where smoke from a cigarette disperses within a room at low air exchange rate and under natural convection motion. The characteristic mixing time is determined for some concrete heat sources. A good overview of modeling ventilation flows in an enclosure and methods of solution is presented in [10, 11, 12]. As indicated in [12], CFD models occupy 70 percents of the works related to the ventilation performance in buildings. Three patterns of mixed convection in a two-dimensional room: steady, periodic and oscillatory are reported in [13], [14] and [15]. At moderate rate of the ventilation the Grashof number, that express the heat flux intensity, does determine the pattern of the flow. The removal of heat or and contaminant as the main applied target of the studies is considered in series of works. The way of introducing heat and contaminants into enclosure is diverse as well as the inlet-outlet location. In [16] a contaminant is supplied to a two-dimensional room through an inlet with air stream, while in [17] a contaminant is assumed to be initially uniformly distributed in a box. In [18] a "cool" source of a contaminant locates at the center of a three-dimensional enclosure. A two-dimensional room model with a "hot" source of contaminant on the bottom side is considered in [15], [19]. In [20] a heat source and a contaminant one are separated in a two-dimensional room. The results of the all mentioned studies show that the contaminant removal efficiency clearly depends on the location of the contaminant source as well as the outlet arrangement.

Nomenclature	
L: Cub length	*Greek symbols:*
g: Gravitational acceleration	v: Kinematic viscosity
Gr: Grashof number ($=g\beta\Delta TL^3/v^2$)	α: Thermal diffusivity
Gr_c: Grashof number ($=g\beta_c\Delta CL^3/v^2$)	α_c: Mass diffusivity
Pr: Prandtl number ($=v/\alpha$)	β: Coefficient of thermal expansion
Ra: Rayleigh number (=Gr.Pr)	β_c: Coefficient of mass expansion
Sc: Schmidt number ($=v/\alpha_c$)	ρ_0: Reference density
Re: Reynolds number (=UL/v)	$\Omega=(\Omega^x, \Omega^y, \Omega^z)$: Dimensionless vector of vorticity
Nu: Nusselt number	ΔT: Characteristic temperature
Sh: Sherwood number	ΔC: Characteristic contaminant concentration
U: Characteristic velocity	
u,v,w: Dimensionless velocity components	
p: Pressure	
T: Dimensionless temperature	
C: Dimensionless contaminant	
Si: Inlet area	
So: Outlet area	
k_T: Coefficient of heat conductivity	
k_C: Coefficient of mass conductivity	
x,y,z: Dimensionless Cartesian coordinates	

In this paper our concern focuses on the total influence of complex factors such as the heterogeneous heat flux on the box bottom, the hot level of the contaminant source, the Reynolds and the Grashof number of heat and contaminant, and the inlet-outlet location on the contaminant removal efficiency.

II. The Problem Formulation

Our numerical simulation will be carried out on the base of the Boussinesq approximation of the Navier-Stokes equations [6], [21], [22]:

$$\begin{cases} \dfrac{\partial \vec{V}}{\partial t} + \left(\vec{V}.\nabla\right)\vec{V} = -\dfrac{1}{\rho_0}\nabla p + \nu\Delta\vec{V} + \left(g\beta T' + g\beta_c C'\right)\vec{k} \\ div\vec{V} = 0 \\ \dfrac{\partial T'}{\partial t} + \left(\vec{V}.\nabla\right)T' = \alpha\Delta T' \\ \dfrac{\partial C'}{\partial t} + \left(\vec{V}.\nabla\right)C' = \alpha_c\Delta C' \end{cases}$$

Taking *U, L, ΔT, ΔC* as the characteristic velocity, length, temperature and contaminant respectively, and making all variables in the above equations non-dimensional we have [22]:

$$\frac{\partial u}{\partial t} + u\frac{\partial u}{\partial x} + v\frac{\partial u}{\partial y} + w\frac{\partial u}{\partial z} = -\frac{\partial p}{\partial x} + \frac{1}{\mathrm{Re}}\left(\frac{\partial^2 u}{\partial x^2} + \frac{\partial^2 u}{\partial y^2} + \frac{\partial^2 u}{\partial z^2}\right) \quad (1)$$

$$\frac{\partial v}{\partial t} + u\frac{\partial v}{\partial x} + v\frac{\partial v}{\partial y} + w\frac{\partial v}{\partial z} = -\frac{\partial p}{\partial y} + \frac{1}{\mathrm{Re}}\left(\frac{\partial^2 v}{\partial x^2} + \frac{\partial^2 v}{\partial y^2} + \frac{\partial^2 v}{\partial z^2}\right) \quad (2)$$

$$\frac{\partial w}{\partial t} + u\frac{\partial w}{\partial x} + v\frac{\partial w}{\partial y} + w\frac{\partial w}{\partial z} = -\frac{\partial p}{\partial z} + \frac{1}{\mathrm{Re}}\left(\frac{\partial^2 w}{\partial x^2} + \frac{\partial^2 w}{\partial y^2} + \frac{\partial^2 w}{\partial z^2}\right) + \frac{Gr}{\mathrm{Re}^2}T + \frac{Gr_c}{\mathrm{Re}^2}C \quad (3)$$

$$\frac{\partial u}{\partial x} + \frac{\partial v}{\partial y} + \frac{\partial w}{\partial z} = 0 \quad (4)$$

$$\frac{\partial T}{\partial t} + u\frac{\partial T}{\partial x} + v\frac{\partial T}{\partial y} + w\frac{\partial T}{\partial z} = \frac{1}{\mathrm{Pr}}\left(\frac{\partial^2 T}{\partial x^2} + \frac{\partial^2 T}{\partial y^2} + \frac{\partial^2 T}{\partial z^2}\right) \quad (5)$$

$$\frac{\partial C}{\partial t} + u\frac{\partial C}{\partial x} + v\frac{\partial C}{\partial y} + w\frac{\partial C}{\partial z} = \frac{1}{Sc}\left(\frac{\partial^2 C}{\partial x^2} + \frac{\partial^2 C}{\partial y^2} + \frac{\partial^2 C}{\partial z^2}\right) \quad (6)$$

Note that all the variables in (1)-(6) are now dimensionless. The boundary conditions for equations (1)-(6) will be discussed later. Now we rewrite (1), (2) and (3) in the vorticity variable introducing the vorticity vector by the form:

$$\vec{\Omega}\left(\Omega^x, \Omega^y, \Omega^z\right) = rot\vec{V},\ \Omega^x = \frac{\partial w}{\partial y} - \frac{\partial v}{\partial z},\ \Omega^y = \frac{\partial u}{\partial z} - \frac{\partial w}{\partial x},\ \Omega^z = \frac{\partial v}{\partial x} - \frac{\partial u}{\partial y} \quad (*)$$

By differentiating (1), (2) and (3) with respect to appropriate spatial variable and taking account of (4), we have:

$$\Omega^x_t + u\Omega^x_x + v\Omega^x_y + w\Omega^x_z - \Omega^x u_x - \Omega^y u_y - \Omega^z u_z - \frac{1}{\mathrm{Re}}\left(\Omega^x_{xx} + \Omega^x_{yy} + \Omega^x_{zz}\right) = \frac{Gr}{\mathrm{Re}^2}T_y + \frac{Gr_c}{\mathrm{Re}^2}C_y \quad (7)$$

$$\Omega^y_t + u\Omega^y_x + v\Omega^y_y + w\Omega^y_z - \Omega^x v_x - \Omega^y v_y - \Omega^z v_z - \frac{1}{\mathrm{Re}^2}\left(\Omega^y_{xx} + \Omega^y_{yy} + \Omega^y_{zz}\right) = -\frac{Gr}{\mathrm{Re}^2}T_x - \frac{Gr_c}{\mathrm{Re}^2}C_x \quad (8)$$

$$\Omega^z_t + u\Omega^z_x + v\Omega^z_y + w\Omega^z_z - \Omega^x w_x - \Omega^y w_y - \Omega^z w_z - \frac{1}{\mathrm{Re}^2}\left(\Omega^z_{xx} + \Omega^z_{yy} + \Omega^z_{zz}\right) = 0 \quad (9)$$

Next, by the differentiation and transformation of (4) one can get the following equations for the velocity components:

$$u_{xx} + u_{yy} + u_{zz} = \Omega^y_z - \Omega^z_y \quad (10)$$

$$v_{xx} + v_{yy} + v_{zz} = \Omega^z_x - \Omega^x_z \quad (11)$$

$$w_{xx} + w_{yy} + w_{zz} = \Omega^x_y - \Omega^y_x \quad (12)$$

In (7)-(12) subscript letters mean variables with respect to which the differential is taken.

These equations will be integrated for determining the vector of vorticity and velocity. Fig. 1 indicates the enclosure considered in this paper. It is a box of length *L* that in the non-dimensional form is the unit box.

We denote the sides of the box by $S_T, S_B, S_L, S_R, S_F, S_K$ for top, bottom, left, right, front and back respectively. Now for the system of equations (5)-(12) the boundary conditions are set as follows. For velocity components:

$$u = v = w\big|_{all\ sides} = 0 \tag{13a}$$

$$u = v = w\big|_{all\ sides - Si - So} = 0;\ \text{on } Si: v = w = 0, u = 1;\ \text{on } So: v = w = 0, u = Si / So \tag{13.b}$$

$$u = v = w\big|_{all\ sides - Si - So} = 0;\ \text{on } Si: u = w = 0, v = 1;\ \text{on } So: u = w = 0, v = Si / So \tag{13c}$$

where (13a) is applied to the natural convection problem, (13b) to the mixed convection with the inlet on the left side, the outlet on the right one, (13c) to the case when the ventilation flow is directed from the face side to the back.

From the definition (*) and (13) boundary conditions for vorticity components are set as follows:

$$\Omega^x\big|_{S_l, S_R} = 0, \Omega^x\big|_{S_F, S_B} = w_y,\ \Omega^x\big|_{S_B, S_T} = -v_z \tag{14}$$

$$\Omega^y\big|_{S_F, S_K} = 0, \Omega^y\big|_{S_L, S_R} = -w_x,\ \Omega^y\big|_{S_B, S_T} = u_z \tag{15}$$

$$\Omega^z\big|_{S_B, S_T} = 0, \Omega^z\big|_{S_L, S_R} = v_x,\ \Omega^z\big|_{S_F, S_K} = -u_y \tag{16}$$

To study the influence of the heat inhomogeneity at the bottom side on the contaminant spreading we divide the box base into several parts along the axis *Ox* (Fig.1). The area ratio of S_1, S_2, S_3, and S_4 to the base are 1/16, 3/8, 3/8 and 3/16 respectively. The contaminant source occupies whole central part S_1. Now for energy and contaminant we impose the following conditions:

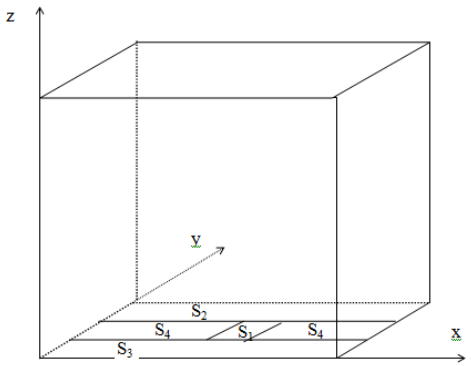

Fig. 1 the box and its base divided into domains with different boundary conditions for temperature and contaminant

$$T_n = C_n\big|_{S_F + S_K + S_L + S_R + S_T} = 0 \tag{17a}$$

$$T_n = C_n\big|_{S_F + S_K + S_L + S_R + S_T - Si - So} = 0,\ T = C\big|_{Si} = 0,\ T_n\big|_{So} = k_T\left(T\big|_{So} - T\big|_{out}\right),\quad C_n\big|_{So} = k_C\left(C\big|_{So} - C\big|_{out}\right) \tag{17b}$$

$$T_n\big|_{S_2} = -1, T\big|_{S_3, S_4} = 0 \tag{18}$$

$$C_n\big|_{S_2, S_3, S_4} = 0, C_n\big|_{S_1} = -1 \tag{19}$$

$$T\big|_{S_1} = 1 \tag{20a}$$

$$T\big|_{S_1} = 0 \tag{20b}$$

where (17a) is used for the natural convection case while (17b) for mixed convection one. In line with (18), domain S_2 is hot while S_3 and S_4 are cool. Condition (20a) and (20b) mean that the contaminant source S_1 is "hot" and "cool" respectively. It is worth discussing the imposition of the outlet condition for both energy and contaminant. Almost works relevant to numerical simulating the heat-contaminant removal from a ventilated enclosure have applied the no-flux condition for all the variables at the outlet. In fact this condition is of mathematical nature rather than physical. Such condition is usually set on a boundary of a computational domain where the perturbation imposed by a submerged object on a uniform fluid flow can be ignored so all the variables of the flow may be assumed to be uniform again. For our problem this condition is hardly confirmed on the outlet. Meantime (17b) is the general condition for energy so it is more reasonable for our problem. On

the other side (17b) assists the calculating the total heat or contaminant expelled through the outlet via the Nusselt or Shewood number respectively. Theses values, as known, are calculated as the integral of heat or contaminant flux over the outlet. So one has:

$$Nu = \iint_{So} -T_n ds; \quad Sh = \iint_{So} -C_n ds \qquad (**)$$

Thus the problem of natural convection flow with a contaminant source in a box consists of equations (7)-(12) (with *Re*=1), equations (5) and (6), and boundary conditions (13a), (14)-(16), (17a), (18), (19) and (20a) or (20b). For the mixed convection problem the system of governing equations are the same (but with *Re*>1), and the boundary conditions include (13b) or (13c), (17)-(19), (20a) or (20b)

Now for reference, we denote the problem that consists condition (20a) by A-case whilst the problem with (20b) by B-case.

III. The Numerical Method

To integrate the transport equations for vortices (8)-(10) here we apply the ADI and time splitting technique for the finite difference method based on the Samarski scheme [23]. We describe this numerical procedure in detail for equation (8) as follows. We split every time step of the integration (τ) into three sub steps. At the first sub step we integrate equation (8) with all derivatives of Ω^x with respect to variable x in the left part (x-direction):

$$\frac{\left(\Omega^x\right)^{n+1/3} - \left(\Omega^x\right)^n}{\tau/3} + u\left(\Omega^x\right)^{n+1/3}_{\tilde{x}} - 0.5|u|k_1\left\{\Omega^x_x - \Omega^x_{\bar{x}}\right\}^{n+1/3} - a\left(\Omega^x\right)^{n+1/3}_{x\bar{x}} - u_x\left(\Omega^x\right)^{n+1/3} =$$
$$-v\left(\Omega^x\right)^n_{\tilde{y}} - w\left(\Omega^x\right)^n_{\tilde{z}} + u_y\left(\Omega^y\right)^n + u_z\left(\Omega^z\right)^n + \left\{\Omega^x_{y\bar{y}} + \Omega^x_{z\bar{z}}\right\}^n + GrT^n_y + Gr_c C^n_y \qquad (23)$$

At the second sub step the analogous equation for y-direction is integrated:

$$\frac{\left(\Omega^x\right)^{n+2/3} - \left(\Omega^x\right)^{n+1/3}}{\tau/3} + v\left(\Omega^x\right)^{n+2/3}_{\tilde{y}} - 0.5|v|k_1\left\{\Omega^x_y - \Omega^x_{\bar{y}}\right\}^{n+2/3} - b\left(\Omega^x\right)^{n+2/3}_{y\bar{y}} - u_x\left(\Omega^x\right)^{n+2/3} =$$
$$-u\left(\Omega^x\right)^{n+1/3}_{\tilde{x}} - w\left(\Omega^x\right)^{n+1/3}_{\tilde{z}} + u_y\left(\Omega^y\right)^n + u_z\left(\Omega^z\right)^n + \left\{\Omega^x_{x\bar{x}} + \Omega^x_{z\bar{z}}\right\}^{n+1/3} + GrT^n_y + Gr_c C^n_y \qquad (24)$$

And finally, at the third sub step the equation for z-direction is solved:

$$\frac{\left(\Omega^x\right)^{n+1} - \left(\Omega^x\right)^{n+2/3}}{\tau/3} + w\left(\Omega^x\right)^{n+1}_{\tilde{z}} - 0.5|w|k_1\left\{\Omega^x_z - \Omega^x_{\bar{z}}\right\}^{n+1} - c\left(\Omega^x\right)^{n+1}_{z\bar{z}} - u_x\left(\Omega^x\right)^{n+1} =$$
$$-u\left(\Omega^x\right)^{n+2/3}_{\tilde{x}} - v\left(\Omega^x\right)^{n+2/3}_{\tilde{y}} + u_y\left(\Omega^y\right)^n + u_z\left(\Omega^z\right)^n + \left\{\Omega^x_{x\bar{x}} + \Omega^x_{y\bar{y}}\right\}^{n+2/3} + GrT^n_y + Gr_c C^n_y \qquad (25)$$

In (23)-(25) we denote:

$$\left(f_x\right)_{ijk} = \left(f_{i+1,jk} - f_{ijk}\right)/h_i; \ \left(f_{\bar{x}}\right)_{ijk} = \left(f_{ijk} - f_{i-1,jk}\right)/h_{i-1}; \ \left(f_{\tilde{x}}\right)_{ijk} = 0.5\left(f_x + f_{\bar{x}}\right);$$
$$\left(f_{x\bar{x}}\right)_{ijk} = 2\left(f_x - f_{\bar{x}}\right)/\left(h_{i-1} + h_i\right); \ h_i = x_{i+1} - x_i; \ a = 1/\left(1 + |u_{ijk}|k_2 h_i \,\mathrm{Re}\right); \qquad (26)$$
$$b = 1/\left(1 + |v_{ijk}|k_2 h_i \,\mathrm{Re}\right); c = 1/\left(1 + |w_{ijk}|k_2 h_i \,\mathrm{Re}\right)$$

where f stands for any component of velocity or the voticity vector.

The analogous procedure is applied for integrating equations (9) and (10). It is obviously from (26) that the central scheme for both the first and second derivatives results in the case when $k_1 = k_2 = 0$ while in the case with $k_1 = 1, k_2 = 0$ one has the upwind scheme. Finally we have the Samarski scheme [10], [11] taking $k_1 = k_2 = 1$. In this paper the last scheme is applied.

To calculate the solution of (10)-(12) the second order central finite difference scheme is used for the Laplace operator and the multigrid method [24], [25], and [26] is applied to solve the system of finite difference equations. The multigrid method extremely reduces the computational time of our numerical simulation.

IV. Numerical Results And Discussion

4.1 The contaminant spreading with buoyancy

The numerical simulation in this paper is carried out for the case when the contaminant-carbon dioxide spreads by the natural convection in a box filled with the air. The Grashof number (*Gr*) ranges from 10^4 to 5.10^5,

and *Grc* is fixed at value 10^5. The common fixture that our simulation shares with the other studies mentioned in the introduction of this paper is the existence of the steady air flow at moderate Grashof number despite the fact that the boundary condition for heat in our case is much different from that imposed in the mentioned works. Moreover the natural convective motion in our study also includes contaminant spreading process. The recording flow parameters at a series of time moments in three points P1(0.5,0.5,0.175), P2(0.5,0.5,0.5) and P3(0.5,0.5,0.875) helps to determine the time evolution of the motion. In Fig. 2 we show the change by time of the *w*-velocity component at point P2 (the center of the box) for several Grashof numbers. It is interesting to note that condition (20) has a clear effect on the kind of the convective motion in our problem formulation. At $Gr=2.10^4$ the convective motion in both cases A and B, as indicated in Fig. 2, becomes stationary after a relatively short time interval. At $Gr=2.10^5$, the flow in A-case ("hot" contaminant source) has clearly fluctuated by time whilst for B-case ("cool" contaminant source) a strictly time periodic solution is resulted. This kind of time periodic flow for natural convection in enclosures was recognized in studies [13, 14] and [15]. At larger Grashof number ($Gr=3.10^5$) for B-case an unsteady motion is resulted. Our simulation also shows that when the Grashof number increases both the amplitude of the flow fluctuation and its frequency become lager. It should note that the behavior of *w*-component as shown in Fig. 2 is common for all the remain parameters of the flow such as *u*- and *v*-components of the velocity, temperature, and contaminant in point P1, P2, and P3.

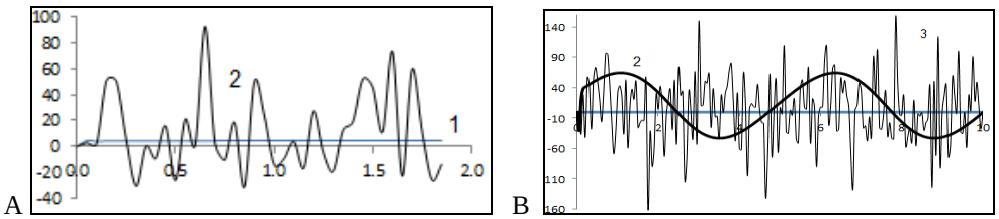

Fig. 2 *w*-velocity component in point P2 at $Grc=10^5$
A-case (1: $Gr=2.10^4$, 2: $Gr=2.10^5$); B-case (1: $Gr=2.10^4$, 2: $Gr=2.10^5$, 3: $Gr=3.10^5$)

The effect of the boundary condition (20) on the amount of the contaminant released from the source S_1 is shown in Fig. 3. This amount in A-case ("hot" contaminant source) is nearly ten times bigger than that of B-case ("cool" source). This is reasonable because heat always assists the emission and spreading contaminant. The temperature distribution on the symmetrical axis of the box also clearly indicates the influence of the heat condition (20) imposed at the source. As shown in the left part of Fig. 3 for A-case one has $T_1 > T_2 > T_3$ while for B-case $T_2 > T_1 > T_3$. This result is reasonable too because in A-case hot air rises directly from S_1 domain while in B-case the air layer adjacent to S_1 is always relatively cool due to the effect of the Rayleigh-Taylor stability.

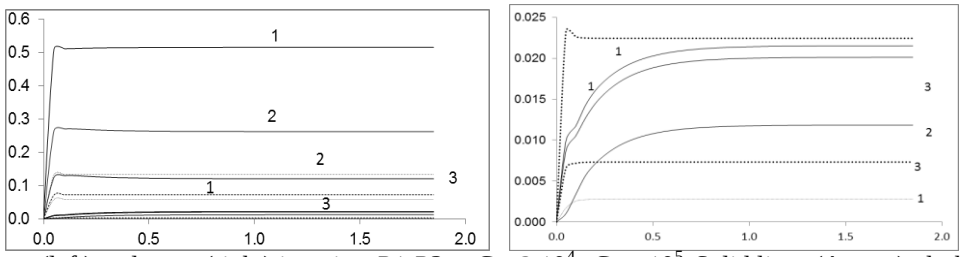

Fig. 3 temp. (left) and cont. (right) in points P1-P3 at $Gr=2.10^4$, $Grc=10^5$. Solid lines (A-case), dash lines (B-case)

Finally the boundary condition (20) also strongly effects on the structure of the air flow in the box. This can be seen in Fig. 4 where shown the velocity field on the middle horizontal section of the cube. The complex structure of the natural convection in the box caused by a complicated boundary condition for heat on the cube base can be demonstrated in Fig. 5. As shown in [6] for the natural convection in a box heated from below there are four different stable structures. In our case the convective structure is more complex because of the inhomogeneity of heat boundary condition on the box bottom.

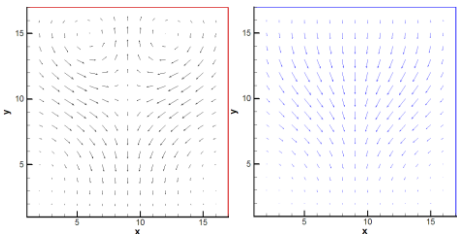

Fig. 4 velocity field on section z=0.5 at $Gr=2.10^4$ $Grc=10^5$ in A-case (left) and B-case (right)

Next our attention focuses on the contaminant distribution in the box when its base is heterogeneously heated from below that is expressed by boundary conditions (18) and (20). The results of the simulation of this study indicate that if the contaminant is discharged continuously from source S_1 then at any moment the contaminant density is in proportion to the intensity of the heat flux below. It means that the contaminant distribution on any horizontal section of the box follows the rule that the hotter region below the thicker contaminant above. In Fig. 6 the temperature and contaminant distribution on three sections x=0.875, z=0.125 and z=0.875 is presented. It is necessary to remind that the hot region at the box base arranges within $0 \le x \le 1,\ 0.625 \le y \le 1$ while the cool one takes $0 \le x \le 1, 0 \le y \le 0.625$. Note that the temperature distribution on any horizontal section, as seen in Fig. 6, correctly reflects the location of heat sources on the bottom. Fig. 6 also shows that both the contaminant and temperature distribution within the box have the common character mentioned above.

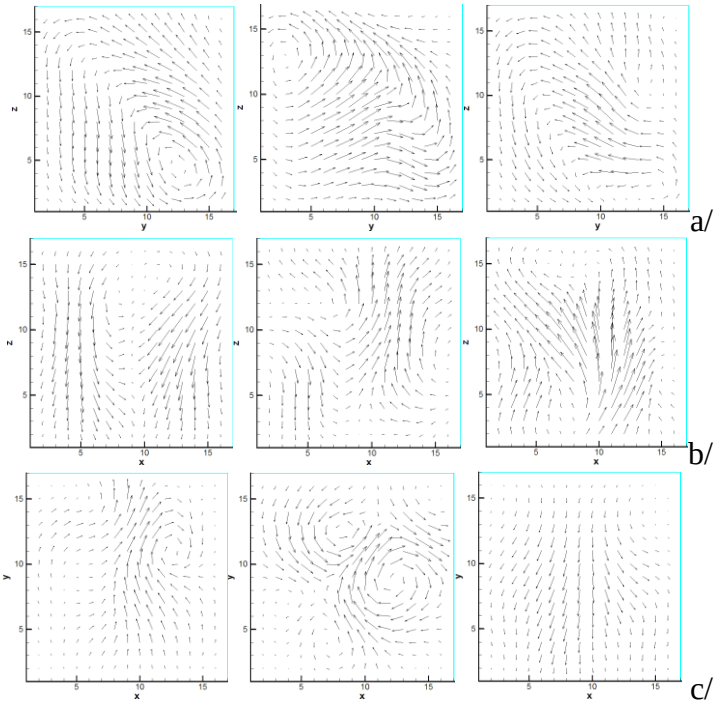

Fig. 5 vector field on: a/ x-sections, x=0.125, x=0.5, x=0.875; b/ y-sections, y=0.125, y=0.5, y=0.875; c/ z-sections, z=0.125, z=0.5, z=0.875 for B-case at Gr=3.10^5, Grc=10^5.

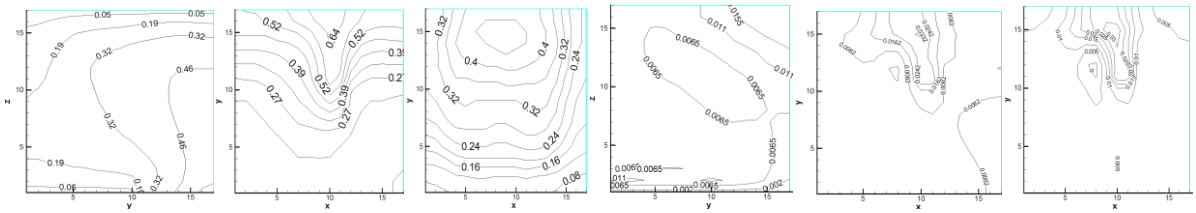

Fig. 6 A-case: isotherms (three first pictures) and contaminant on sections: x=0.875, z=0.125 and z=0.875 respectively for Gr=2.10^5, Grc=10^5.

For the B-case these characteristics of the temperature and contaminant distribution remain the same as for A-case. And this is held for all three types of the flow: steady, periodic and unsteady. This conclusion is demonstrated in Fig. 7.

Fig. 8 shows a picture that illustrates the above conclusion on the way of contaminant spreading in a box in the presence of a natural convective flow caused by a complicated heat condition at the box bottom. In this picture the box bottom is divided into two equal parts. The left part surface is kept cool by ice below while the right part one is heated by a lamp. A point contaminant source locates at the center of the box base. As seen in the picture the smoke always tends to spread more into the hot region of the air in the box.

Fig. 8 experimental illustration of the contaminant spreading in a natural convection in a box.

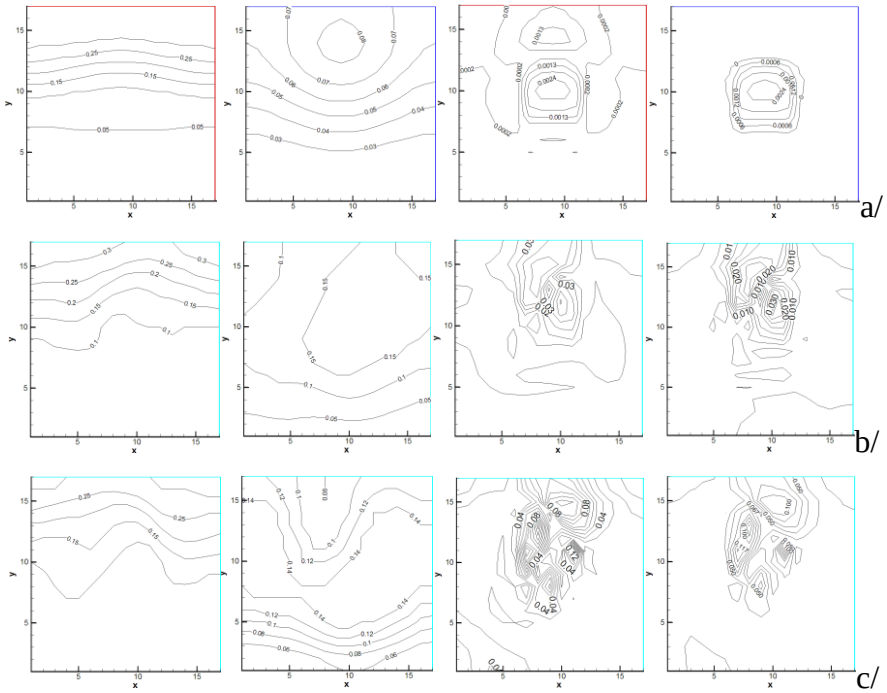

Fig.7 B-case: isotherms (two first pictures of each line) and contaminant on sections: z=0.125 and z=0.875 respectively for a/ steady, b/ periodic, c/ unsteady flow.

4.2 The effect of the inlet-outlet location on the removal of heat and contaminant

Now we impose a ventilation flow on the convective motion discussed in § 4.1. The ventilation system contains one inlet and one outlet that are located on two opposite sides like S_L-S_R or S_F-S_K. For S_L-S_R location the ventilation flow blows from left to right (along x-axis) and for S_F-S_K from front to back (along y-axis). Thereafter we refer these cases as X-X and Y-Y respectively. Both the inlet and outlet are square whose length is L/4. The inlet locates in the middle of the box side at three positions with the height from the floor to its bottom edge is 0, 3L/8 and 3L/4 respectively. These positions are symbolized by letters L, M, H respectively. We consider also three such locations for the outlet on the opposite side. So for both X-X and Y-Y case there are totally eighteen the inlet-outlet configurations. In the future symbol LM means the case of low inlet-middle outlet and etc. In Fig. 8 we show the change by time of u-component of velocity in point P2 (the center of the box) at Re=200 for pure ventilation flow (thin solid line 1), mixed convection of A-case (dash line 2) and mixed convection of B-case (bold solid line 3) at Gr=2.10^5, Grc=10^5. Fig. 9 shows clearly the stabilizing effect of heat convection on low rate ventilation flows. The simulations also show that at the same set of Re, Gr, and Grc the air flow in the box may be steady or unsteady depending on the ventilation direction. In fig. 9 we show the temperature in the center of the box as a function of time. For A-case and for both directions X-X and Y-Y after some time interval the temperature remains unchanged. Whilst for B-case for Y-Y ventilation the temperature clearly varies with time. The results of the simulation indicate that the unsteadiness of the solution of B-case is more sensitive to Re-change than that of A-case. Also Y-Y direction is more sensitive than X-X one for B-case. For A-case the contrary takes place.

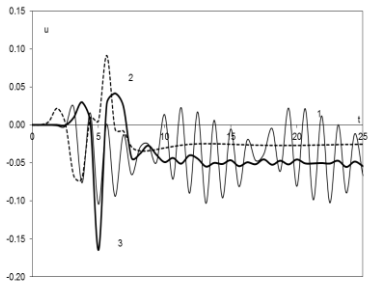

Fig. 8. u-component in point P2 at Re=200, Gr=2.10^5, Grc=10^5. 1: ventilation, 2: mixed convection (A-case), 3: B-case

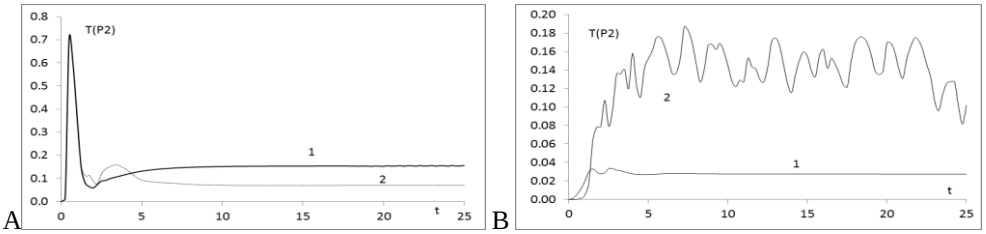

Fig. 9 change by time of temperature in point P2 of A & B case at *Re*=200, *Gr*=2.10^5, *Grc*=10^5, for X-X direction (1) and Y-Y(2).

It is interesting to note that in some cases of the inlet-outlet location the solution of the considered here problem can be a so called multiple-periodic function of time. Fig. 10 shows a such solution for B-case at *Re*=200, *Gr*=2.10^5 and *Grc*=10^5 for LH configuration of X-X ventilation. This solution is likely a periodic function with two time periods. The interaction between ventilation and natural convection in the cube creates complicated air flows whose structure is strongly depends on the direction of the ventilation. Fig. 11 shows the velocity field at the middle horizontal section of the box for some of such flows. The pictures indicate the obvious influence of the ventilation direction on the formation of the resultant flows in both cases A and B.

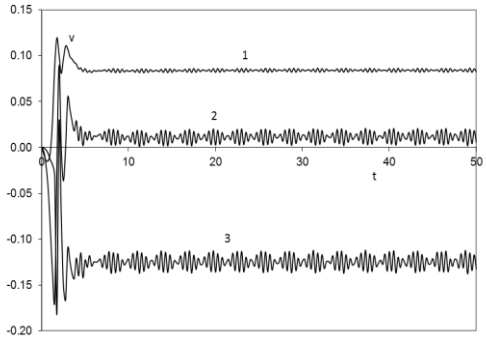

Fig. 10 v- component in points Pk (k) of B-case for LH, X-X, *Re*=200, *Gr*=2.10^5, *Grc*=10^5.

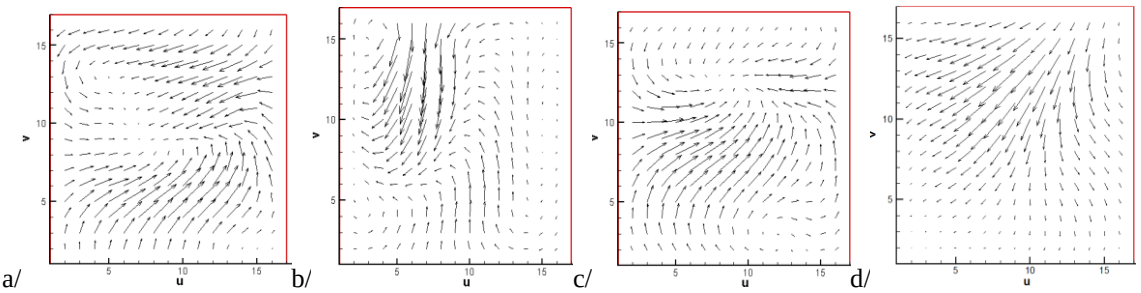

Fig11 Velocity field at z=0.5 for *Re*=200, *Gr*=2.10^5, *Grc*=10^5: A-case (a/ X-X, b/ Y-Y), B-case (c/ X-X, d/ Y-Y)

Thus as indicated in [13], [14], [15] and by this study, natural convection may make an unsteady ventilated flow in an enclosure steady or pseudo steady at low ventilation rate. The next purpose of this paper is to elucidate the effect of the inlet-outlet configuration on the efficiency of heat and contaminant removal from the box. The answer to this problem has a big practical application. As indicated above, here the simulations are carried out for 18 inlet-outlet configurations for each case A and B. For every configuration the Nusselt and Shewood number are calculated by (**). The efficiency of any configuration expressed by the ratio of *Nu* and *Sh* of this configuration to *Nu* and *Sh* of LL location respectively is provided in table 1. The cases with both ratios greater than unit are marked by bold numbers in two corresponding columns for Nu/Nu and Sh/Sh . These cases have a more removal efficiency for both heat and contaminant in the comparison with the lowest inlet-outlet location. The bold italic numbers in column Sh/Sh mark the case with a better contaminant removal only.

I-O	Re=150, Gr=2.10^5, Grc=10^5								Re=200, Gr=2.10^5, Grc=10^5							
	A-case				B-case				A-case				B-case			
	X-X		Y-Y		X-X		Y-Y		X-X		Y-Y		X-X		Y-Y	
	Nu/Nu	Sh/Sh	Nu/Nu	Sh/Sh	Nu/Nu	Sh/Sh	Nu/Nu	Sh/Sh	Nu/Nu	Sh/Sh	Nu/Nu	Sh/Sh	Nu/Nu	Sh/Sh	Nu/Nu	Sh/Sh
LL	1.00	1.00	1.00	1.00	1.00	1.00	1.00	1.00	1.00	1.00	1.00	1.00	1.00	1.00	1.00	1.00
LM	0.40	0.99	0.38	0.44	0.44	0.11	0.62	0.45	0.32	0.88	0.52	0.78	1.12	0.47	0.58	***1.21***
LH	0.16	0.86	0.05	0.57	0.13	0.03	0.14	0.31	0.24	0.33	0.04	0.68	0.20	0.52	0.06	0.23
ML	0.99	0.97	**1.00**	**1.00**	0.94	***1.63***	**1.05**	**1.00**	0.99	0.97	**1.00**	**1.01**	**1.01**	**1.23**	**1.02**	**1.00**
MM	0.52	0.57	0.37	0.43	0.88	***3.03***	0.61	0.49	0.42	0.61	0.55	0.73	1.19	0.37	0.68	***1.35***
MH	0.15	0.58	0.05	0.50	0.13	0.01	0.16	0.29	0.18	0.25	0.06	0.67	0.96	0.32	0.06	0.20
HL	**1.01**	**1.02**	**1.00**	**1.02**	**1.06**	**1.04**	0.98	0.97	**1.00**	**1.01**	**1.00**	**1.02**	**1.07**	**16.36**	0.99	0.98
HM	0.43	***1.30***	0.40	0.49	0.39	0.11	0.71	0.57	0.37	***1.3***	0.05	0.74	**5.46**	**1.56**	0.63	***1.19***
HH	0.19	0.93	0.05	0.49	0.15	0.003	0.15	0.29	0.26	0.25	0.04	0.60	0.001	1.02	0.07	0.22

Table 1. Heat and contaminant removal of different inlet-outlet locations in comparison with LL case

The results in table 1 indicate that at low ventilation rates for X-X direction configurations LL, HL would be good choices for both cases, and HL and HM may be very good for B-case at a larger the Reynolds number. For Y-Y ventilation direction configurations LL, ML and HL are nearly equivalent by the removal efficiency. If the contaminant removal is the main concern then configurations LM, MM and HM would be the first choice in this case.

I-O	Re=150, Gr=2.10^5, Grc=10^5				Re=200, Gr=2.10^5, Grc=10^5			
	A-case, X-X/Y-Y		B-case, X-X/Y-Y		A-case, X-X/Y-Y		B-case, X-X/Y-Y	
	Nu/Nu	Sh/Sh	Nu/Nu	Sh/Sh	Nu/Nu	Sh/Sh	Nu/Nu	Sh/Sh
LL	0.16	0.82	0.39	6.49	0.25	1.01	0.31	0.39
LM	0.17	1.87	0.27	1.63	0.16	1.14	0.60	0.15
LH	0.49	1.23	0.36	0.69	1.46	0.50	0.98	0.89
ML	0.16	0.79	0.35	10.54	0.25	0.98	0.31	0.48
MM	0.22	1.08	0.56	40.52	0.19	0.85	0.54	0.11
MH	0.54	0.94	0.32	0.27	0.82	0.38	5.33	0.65
HL	0.16	0.82	0.42	6.94	0.25	1.00	0.34	6.57
HM	0.17	2.17	0.21	1.24	1.88	1.79	2.68	0.51
HH	0.62	1.54	0.38	0.06	1.59	0.42	0.004	1.78

Table 2. Comparison of the removal efficiency between X-X and Y-Y ventilation direction

To compare the removal efficiency between X-X and Y-Y ventilation direction we divide *Nu* and *Sh* for every corresponding inlet-outlet location. The results are shown in table 2. At *Re*=150, the air flow in the all 36 configurations are steady or nearly steady. So the heat amount removed by Y-Y ventilation is always larger than that of by X-X one for every inlet-outlet configuration. It is appropriate because, in accordance with the heat sources location indicated in Fig. 1, the ventilation flow in Y-Y direction involves more "hot" air than that in X-X direction. Concerning the contaminant removal for A-case three configurations with the lowest outlet are less efficient whilst for B-case such configurations turn out to be with the highest outlet. Generally at low rate ventilation for the considered here problem the X-X ventilation is the best choice.

At *Re*=200 for some inlet-outlet configurations the flow becomes unsteady. Generally the velocity fluctuation assists the temperature diffusion. So, as expected, at the same conditions the unsteady flow expels more heat than the steady. The simulation results show that for three configurations LH, HM, HH of A-case and for MH, HM of B-case the fluctuation of the flow parameters of X-X ventilation is larger than that of Y-Y ventilation. This causes the values at the intersections of the sixth column of table 2 with rows number 6, 11 and 12 exceeding unit. Analogously for B-case the values at the crossing of the eighth column with the ninth and eleventh rows are larger than unit. The simulation results shown in table 2 indicate also that unlike the case of *Re*=150 when X-X ventilation has the obvious advantage over Y-Y, at *Re*=200 for every direction of X-X and Y-Y there exist some very good configurations.

Finally we compare the amount of heat and contaminant removed from the box in A-case with that in B-case. The comparison is provided in table 3.

I-O	Re=150, Gr=2.10^5, Grc=10^5				Re=200, Gr=2.10^5, Grc=10^5			
	A/B, X-X		A/B, Y-Y		A/B, X-X		A/B, Y-Y	
	Nu/Nu	Sh/Sh	Nu/Nu	Sh/Sh	Nu/Nu	Sh/Sh	Nu/Nu	Sh/Sh
LL	1.89	1.26	4.59	10.00	2.72	22.66	3.32	8.76
LM	1.72	11.02	2.78	9.63	0.78	41.97	3.00	5.68
LH	2.32	33.01	1.69	18.61	3.33	14.65	2.24	26.09
ML	2.00	0.75	4.40	10.00	2.66	17.93	3.28	8.84
MM	1.12	0.24	2.78	8.88	0.95	37.36	2.65	4.72
MH	2.19	59.16	1.30	17.01	0.51	17.81	3.34	30.20
HL	1.79	1.24	4.70	10.52	2.51	1.40	3.37	9.18
HM	2.12	15.12	2.59	8.60	0.18	18.93	0.26	5.44
HH	2.39	27.23	1.45	17.13	9.73	5.54	1.99	23.40

Table 3. Comparison of heat and contaminant removed in two cases A and B.

The results in table 3 show that the removal contaminant in A-case ("hot" source of contaminant) is larger than that in B-case ("cool" source) at any configuration and for both values of *Re*. This is appropriate to the fact that temperature always accelerates the releasing contaminant. In the most cases of the inlet-outlet location the heat amount removed of A-case is more than that of B-case. It is reasonable because the number of heat source of A-case is larger.

V. Conclusion

The finite difference method and the multigrid technique are applied to simulate the heat and contaminant removal from a box by low air rate ventilation. The contaminant distribution in the box under the influence of convective motion clearly depends on the distribution of the heat on the floor. The heat convection

caused by the heterogeneous heating the box bottom at moderate Grashof number can make a low air rate ventilated flow steady, periodic or unsteady. The type of the flow also depends on the location of the inlet and outlet on two opposite sides of the cub. The simulations for two Reynolds numbers at the same Grashof number show that the heat and contaminant removal efficiency varies with the ventilation rate, the inlet-outlet configuration as well as the direction of the ventilation flow. The removal also depends on the characteristic of the contaminant source. If this source is dual i.e. it ejects both heat and contaminant at the same time then more heat and more contaminant are removed at any time moment than when the source releases contaminant only.

Reference

[1]. G. D. Mallinson, G. De Vahl Davis. ,1977. Three-dimensional natural convection in a box: a numerical study. Journal of Fluid Mechanics, Vol. 83, **01**, 1-31.

[2]. N. C. Markatos, K.A. Pericleous., 1984. Laminar and turbulent natural convection in an enclosed cavity. International J. of Heat and Mass Transfer, Vol. 27, **5**,755-772.

[3]. W. J. Hiller, et al., 1989. Three-dimensional structures in laminar natural convection in a cubic enclosure. Experimental Thermal and Fluid Science, Vol. 2, 01, 34-44.

[4]. T. Fusegi et al., 1991. A numerical study of three-dimensional natural convection in a differentially heated cubical enclosure. International J. of Heat and Mass Transfer, Vol. 34, **6**, 1543-1557.

[5]. R. J. A Janssen, et al., 1993.Transition to time-periodicity of a natural convection flow in a 3D differentially heated cavity. International J. of Heat and Mass Transfer, Vol. 36, **11**, 2927-2940.

[6]. J. PallarEs, et al., 1996. Natural convection in a cubical cavity heated from below at low Rayleigh numbers. International J. of Heat and Mass Transfer, Vol. 39, **15**, 3233-3247.

[7]. Orhan Aydin, Wen-Jei Yang, 2000. Natural convection in enclosures with localized heating from below and symmetrical cooling from sides. International J. of Numerical Methods for Heat & Fluid Flow. Vol. 10, 5, 518-529.

[8]. Hakan F. Oztop, Eiyad Abu-Nada, 2008. Numerical study of natural convection in partially heated rectangular enclosures filled with Nano fluids. International J. of Heat and Mass Transfer, Vol. 29, 1326-1336.

[9]. A. V. Baughman, A. J. Gadgil, W. W. Nazaroff, 1994. Mixing of a point Source Pollutant by Natural Convection Flow within a Room. Indoor Air J., 4,114-122.

[10]. Miao Wang, 2011. Modeling airflow and contaminant transport in enclosed spaces with advanced models. Purdue University.

[11]. Qingyan Chen and Weiran Xu, 2000. Simplified Method for Indoor Airflow Simulation. Proceeding of CLIMA 2000 World Congress, Brussels, Belgium.

[12]. Qingyan Chen, 2009. Ventilation performation prediction for buildings: A method overview and recent applications. Building and Environment, 44, 848-858.

[13]. Li-Chuan Fang, Effect of mixed convection on transient hydrodynamic removal of a contaminant from a cavity, 2003. International J. of Heat and Mass Transfer, 46, 2039-2049.

[14]. Brahim Ben Beya, Taieb Lili, 2007. Oscillatory double-diffusive mixed convection in a two-dimensional ventilated enclosure. International J. of Heat and Mass Transfer, 50, 4540-4553.

[15]. Tran Van Tran, Nguyen Thi Thuy, 2015. The Interaction Between Ventilation and Natural Convection Flows in a Two-Dimensional Enclosure. Proceedings of International Conference on Scientific Computing, CSC'15, Las Vegas, USA. 213-218.

[16]. Gregory Evans, W. Winters, Ralph Greif, 2006. Effects of buoyancy on contaminant transport in room air flows. 13th. Int. Heat Trans. Conf. Australia, p6.270.

[17]. Di Liu, Fu-Yun Zhao, Guang-Fa Tang, 2008. Numerical analysis of two contaminants removal from a three-dimensional cavity. International J. of Heat and Mass Transfer, 51, 378-382.

[18]. D. T. Bolster and P. F. Linden, 2007. Contaminants in ventilated filling boxes. Journal of Fluid Mechanics, 591, 97-116.

[19]. Sumon Saha, Mohammad Nasim Hasan, Iftheker Ahmed Khan, 2009. Double diffusive mixed convection heat transfer inside a vented square cavity. Chemical Engineering Bulletin, 13, 17-24.

[20]. Alsayed A. El-Agouz, Essaied M. Shuia, 2013. The Effect of The Contaminant Source Performance of The Environmental Displacement Ventilation System. Tanta University Bulletin, V2, N15.

[21]. L.D. Landau, E.M. Lifshitz, 1986. Mechanics of continuous mediums. M. Nauka (in Russian).

[22]. V.I. Polezaev et al., 1987. Mathematical modeling of convective heat and mass transfer on the base of Navier-Stokes equation. M. Nauka (in Russian).

[23]. A.A. Samarski, 1971. Introduction to the theory of finite difference method. Nauka, (in Russian).

[24]. W. Hackbusch, 1985. MultiGrid Methods and Applications. Springer-Verlag, Berlin/New York.

[25]. Volker John, Lutz Tobiska, 2000. Numerical performance of smoothers in coupled multigrid methods for the parallel solution of the incompressible Navier-Stokes equation. Int. J. numer. Meth. Fluids. **33**, 453-473.

[26]. U. Ghia, et al., 1982. High-Re Solution for Incompressible Flow Using the Navier-Stokes Equations and a Multigrid Method. Journal of Computational Physics, **48**, 387-411.